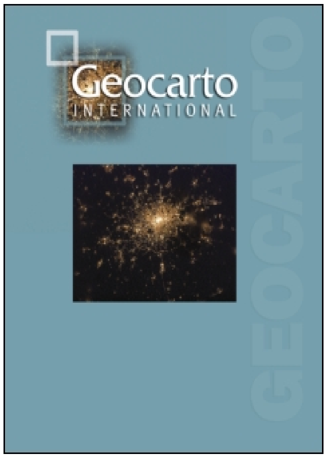

Geocarto International
Publication details, including instructions for authors and subscription information:
http://www.informaworld.com/smpp/title~content=t759156373

Delineation of potential sites for water harvesting structures through remote sensing and GIS techniques: a case study of Kali watershed, Gujarat, India

D. Ramakrishnan [a]; K. H. V. Durga Rao [a]; K. C. Tiwari [a]
[a] Department of Earth Sciences, Indian Institute of Technology, Mumbai, India

Online Publication Date: 01 April 2008
To cite this Article: Ramakrishnan, D., Rao, K. H. V. Durga and Tiwari, K. C. (2008) 'Delineation of potential sites for water harvesting structures through remote sensing and GIS techniques: a case study of Kali watershed, Gujarat, India', Geocarto International, 23:2, 95 - 108
To link to this article: DOI: 10.1080/10106040701417246
URL: http://dx.doi.org/10.1080/10106040701417246

Geocarto International
Vol. 23, No. 2, April 2008, 95–108

Delineation of potential sites for water harvesting structures through remote sensing and GIS techniques: a case study of Kali watershed, Gujarat, India

D. RAMAKRISHNAN*†, K. H. V. DURGA RAO‡ and K. C. TIWARI§

†Department of Earth Sciences, Indian Institute of Technology, Powai, Mumbai 400076, India

‡National Remote Sensing Agency, Balanagar, Hyderabad 500037, India

§Department of Geology, M.S. University of Baroda, Vaodara 390002, India

(*Received in final form 25 April 2007*)

Site suitability studies for check dams, percolation ponds, and subsurface dykes form an integral part of watershed management. This work illustrates the efficacy of remote sensing and GIS tools for identifying suitable sites for these structures. Thematic layers such as land use/land cover, lithology, soils, slope, rainfall and drainage were generated using LISS-III, PAN (IRS-1D), Landsat Thematic Mapper (TM) and collateral data. Runoff potential for different combinations of land use and hydraulic soil groups was computed and classified into three classes. A potential site suitability map for water harvesting/recharging structures was derived following an analytical hierarchy process. The analytically derived potential site suitability map was validated in the field. The accuracy of prediction was estimated on the basis of proximity between derived and field validated sites. In 75% of cases, the sites derived for check dam, percolation pond and subsurface dyke were accurate.

Keywords: Watershed management; Remote sensing; GIS

1. Introduction

Water is essential for all life. It is also one of the prime requirements for agriculture, industrial production and domestic uses. Components of precipitation, resolved into soil moisture and groundwater, are the prerequisites for biomass production and social development in dry areas. Lack of water resources is generally a function of large inter-annual and annual fluctuations of rainfall, poor infiltration, low hydraulic conductivity, storitivity and high evaporative demand. Watershed development and management implies an optimum development of water, land and hence biomass so as to meet the people's basic needs in a sustained manner. This calls for reducing the runoff, soil loss and augmentation of infiltration. A reduction in surface runoff can be achieved by constructing

*Corresponding author. Email: ramakrish@iitb.ac.in

Geocarto International
ISSN 1010-6049 print/ISSN 1752-0762 online © 2008 Taylor & Francis
http://www.tandf.co.uk/journals
DOI: 10.1080/10106040701417246

suitable structures or by changes in land management, which in turn will increase infiltration and aid water conservation.

Thus, micro watershed development calls for a detailed understanding and analysis of various interrelated parameters such as land use, soil, soil moisture, slope, rainfall and lithology (Prasad *et al.* 1993, Yusof *et al.* 2000, Cosh *et al.* 2004). Remote sensing and GIS (Geographic Information Systems) are valuable tools for generating and analysing this thematic information (Ouattara *et al.* 2004). In this study, an attempt was made to select suitable sites for various water harvesting/recharging structures in the Kali watershed, Dahod district of Gujarat, using remote sensing and GIS techniques.

2. Study area

The Kali watershed (figure 1), covering about 200 km^2 area is bound between latitudes 22°40′ N–22°52′ N and longitudes 74°20′ E–74°25′ E. This area is characterised by a semi-arid climate with a mean maximum temperature of 40 °C,

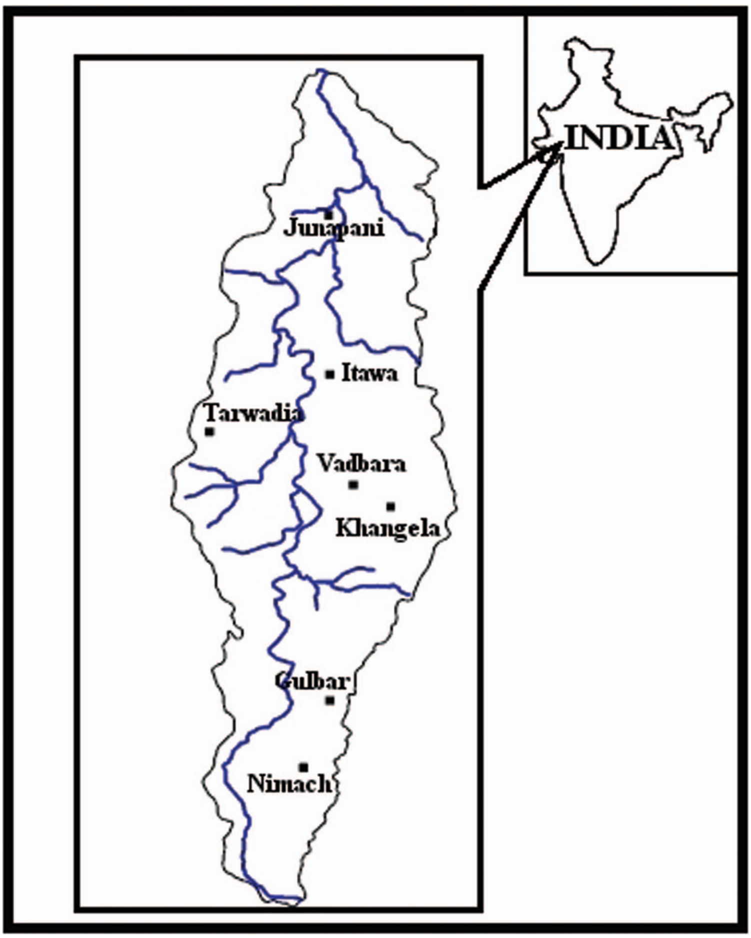

Figure 1. Location map of the study area.

an average annual rainfall of 1000 mm and a high evapotranspiration rate (900 mm). Hard rock controlled undulatory topography with irregular rainfall causes high runoff and poor groundwater potential. Further, scarcity of vegetation accentuates the soil erosion. Thus, the study area calls for an immediate action plan for watershed development.

3. Methodology

The adopted methodology (figure 2) includes a three-tier approach:

1. generation of thematic layers using satellite (IRS-1D-LISS-III, PAN, Landsat Thematic Mapper (TM)) and collateral data;
2. data integration and analysis; and
3. development of decision rules and field validation.

Land use/land cover maps for the period January to December 2000 were generated following standard procedures (maximum likelihood classifier) using ERDAS Imagine software. An existing database (1:250 000 scale) on lithology and soil was upgraded to 1:50 000 scale using Landsat TM data (by image ratios and principal component analysis). The average weighted rainfall for the entire watershed area was computed from the collateral data by the Theissen polygon method. Water balance components were computed in MS-Excel software (www.microsoft.com) following the procedures of Dunne and Leopold (1978). The integration of vector coverages and collateral data was carried out using ARCInfo software (www.arcinfo.com). An analytical hierarchy process (Saaty and Vargas 1991) was adopted to assign weight to parameters that govern the site suitability for water harvesting/recharging structures. Specifications prescribed by the Integrated Mission for Sustained Development (IMSD 1995) and the Food and Agriculture Organization (FAO 1977) were adhered to for site selection.

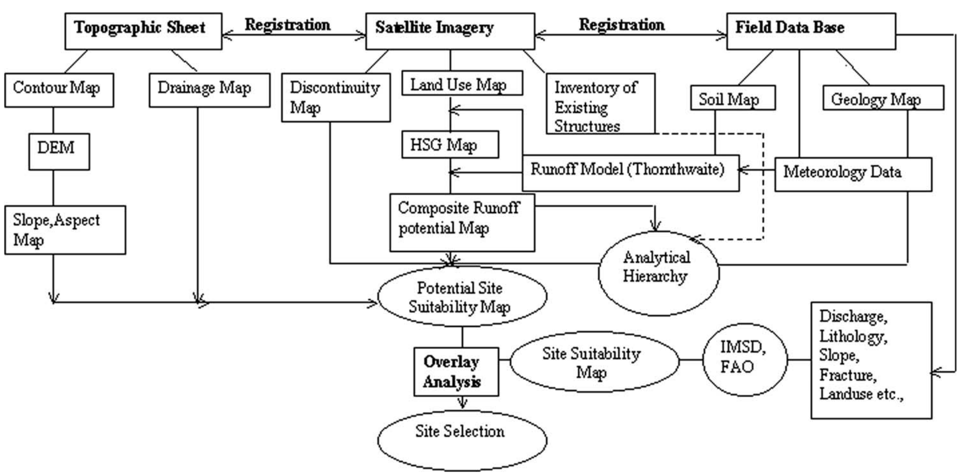

Figure 2. Flow chart depicting the methodology adopted.

4. Results and discussion

4.1 *Hydro-geology and aquifer characteristics*

Precambrian meta-sedimentaries such as quartzites, phyllites, mica schists and gneisses of the Aravalli Super Group constitute a major portion (86%) of the investigated area (figure 3). These rocks were overlaid by patchy occurrence (12%) of massive and Bagh limestone in the central and southern parts of the study area. The Deccan traps are mainly confined to the southern portion of the study area (4%) and overlie limestone, quartzite and phyllite. By virtue of competent contrast, the quartzites were thrown up into ridges in the northern and central parts. Being prone to weathering, the phyllites and schists form the shallow pedimentary slopes and valley. The basaltic areas exhibit conspicuous plateau, mesa and butte landform features.

Being a hard rock area, the secondary porosity and permeability form the only source of ground water recharge/discharge. On the basis of the yield and hydraulic conductivity (K), these aquifers were classified into three classes (table 1) such as poor ($K < 20$ m day^{-1}), moderate ($K = 20$–40 m day^{-1}) and good ($K > 60$ m day^{-1}).

4.2 *Hydraulic soil group*

The hydraulic soil group (HSG) of the study area was derived from prevailing National Bureau of Soil Survey (NBSS) soil maps. The soils in the study area (figure 4) can be grouped under four hydraulic soil groups, i.e. groups A, B, C and D. Soil group A is restricted to flood plains and natural levees (2.9 km^2), whereas soil groups B (21.5 km^2) and C (87.3 km^2) were confined to bazadas and pediments, respectively. Soil group D is confined to pediment inselberg complex and barren uplands (88.1 km^2).

4.3 *Land use/land cover*

Since land use is the key component for controlling runoff and evapotranspiration, land use maps for two seasons (February and September 2000) were considered for this study. By integrating these two maps, a composite land use/land cover map (figure 5) was generated for subsequent analysis. In all, six major land use classes, namely open forest (29.6 km^2), irrigated (38.4 km^2), fallow/scrub (89.8 km^2), barren land (38.0 km^2), water bodies (2.3 km^2) and sand (1.8 km^2) were observed.

4.4 *Drainage network*

The drainage network was generated from the prevailing map sources and subsequently updated using satellite data. The streams were ranked by following the procedure of Horton (1945) and buffered for five metres. This layer is significant from the point of view of site selection specifications.

4.5 *Slope*

Slope is one of the key factors in controlling overland and base flows. Further, slope also governs soil detachability and hence land capability. Following the guidelines of

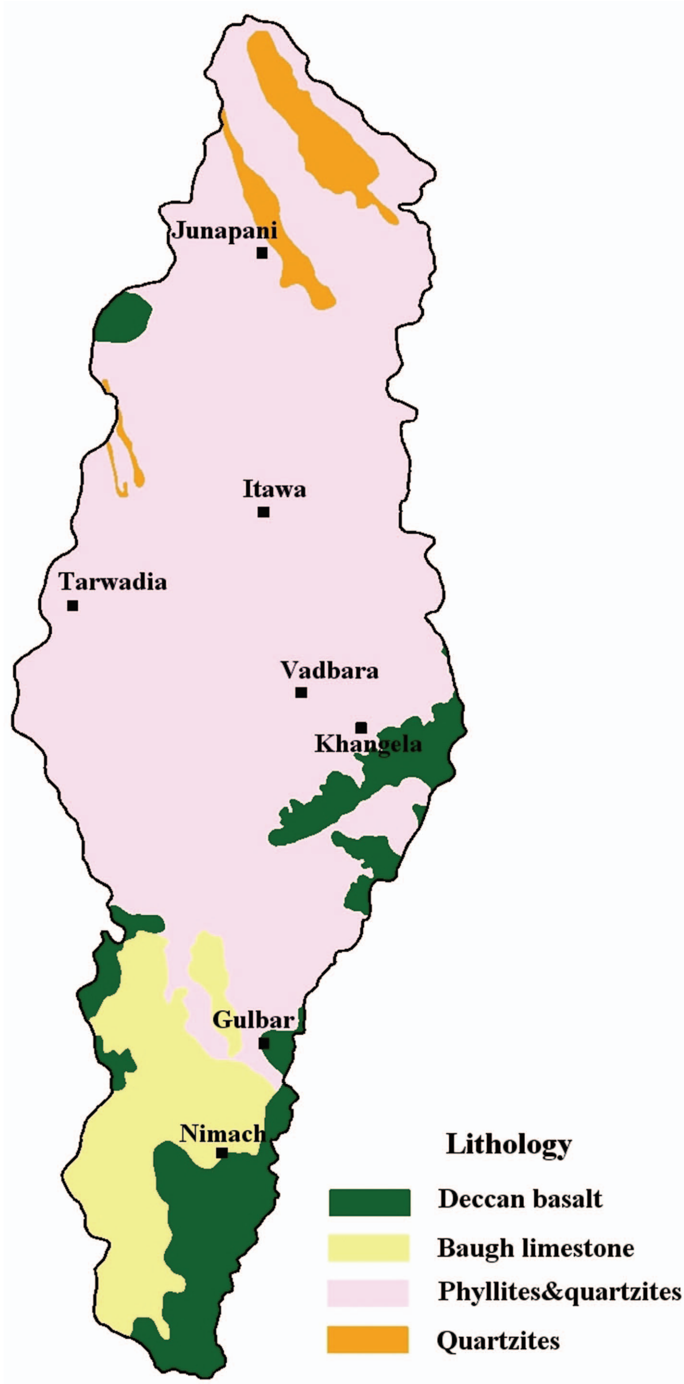

Figure 3. Geology of Kali watershed, Gujarat, India. Available in colour online.

Table 1. Hydro-geological characteristics of rock types in Kali watershed, Gujarat, India.

Litho unit	Area (km^2)	Hydraulic conductivity ($m\ day^{-1}$)	Discharge (lpm)	Class
Slates and phyllites	164.7	<20	100–200	Poor
Bagh beds	12.0	<20	100–300	Poor
Quartzite	8.0	20–40	200–400	Moderate
Traps	15.2	40–60	500–700	Good

the All India Soil and Land Use Survey, seven classes of slope, such as nearly level (0–1%), very gentle (1–3%), gentle (3–5%), moderate (5–10%), strong (10–15), moderately steep (15–35%) and very steep (>35) were derived.

4.6 *Calculation of water balance components*

The water balance of a watershed refers to the balance between precipitation and outflow of water by evapotranspiration, ground water recharge, stream flow and base flow. The water balance of a small drainage basin can be expressed by the general equation:

$$P = I + AET + OF + \Delta SM + \Delta GWS + GWR \quad (1)$$

Where P is the precipitation, I is the infiltration, AET is the actual evapotranspiration, OF is the over land flow, ΔSM is the change in soil moisture, ΔGWS is the change in the ground water storage, and GWR is the ground water runoff.

In this work, AET, OF and ΔSM for different land use classes were computed following the method of Thornthwaite and Mather (1955). Meteorological information on mean monthly rainfall, temperature, wind velocity etc., was collected from field stations. The weighted average precipitation of the watershed was computed following the Thiessen polygon method. Potential evapotranspiration (PET) was calculated using the following equation:

$$PET = 16f(10t_n/J)^a \quad (2)$$

Where PET is the monthly potential evapotranspiration (mm), t_n is the monthly mean temperature (°C), f is a factor to correct for unequal day length between different months, J is the annual heat index, a is the cubic function of J.

$$J = \sum_{1}^{12} j \quad (3)$$

Where j is the monthly heat index obtained by

$$j = (t_n/5)^{1.514} \quad (4)$$

and a is a coefficient obtained by

$$a = (675\times10^{-9})J^3 - (771\times10^{-7})J^2 + (179\times10^{-4})J + 0.492 \quad (5)$$

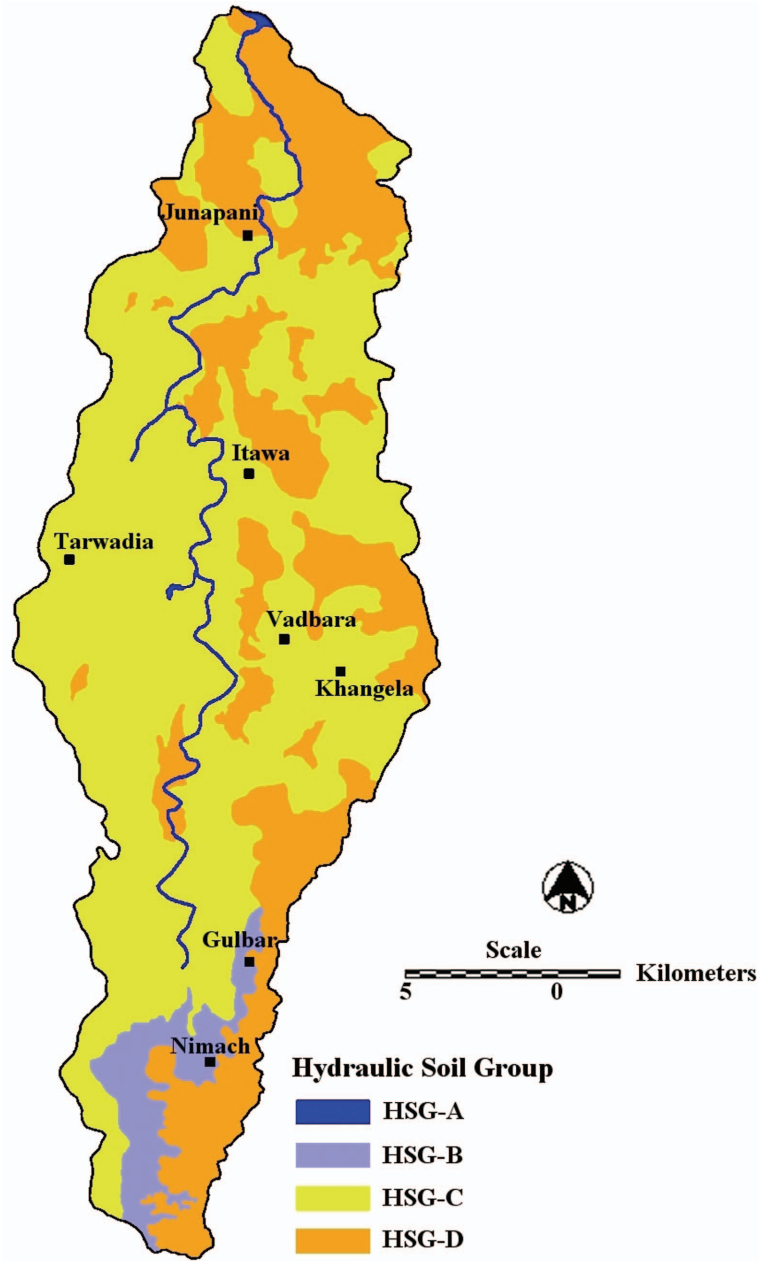

Figure 4. Hydraulic soil group map. Available in colour online.

The value of day length factor *f* was obtained from the readily available charts for different geographic locations.

From the precipitation (*P*) and the potential evapotranspiration (*PET*) values for each month, the difference between *P* and *PET* was calculated. In wet seasons, the

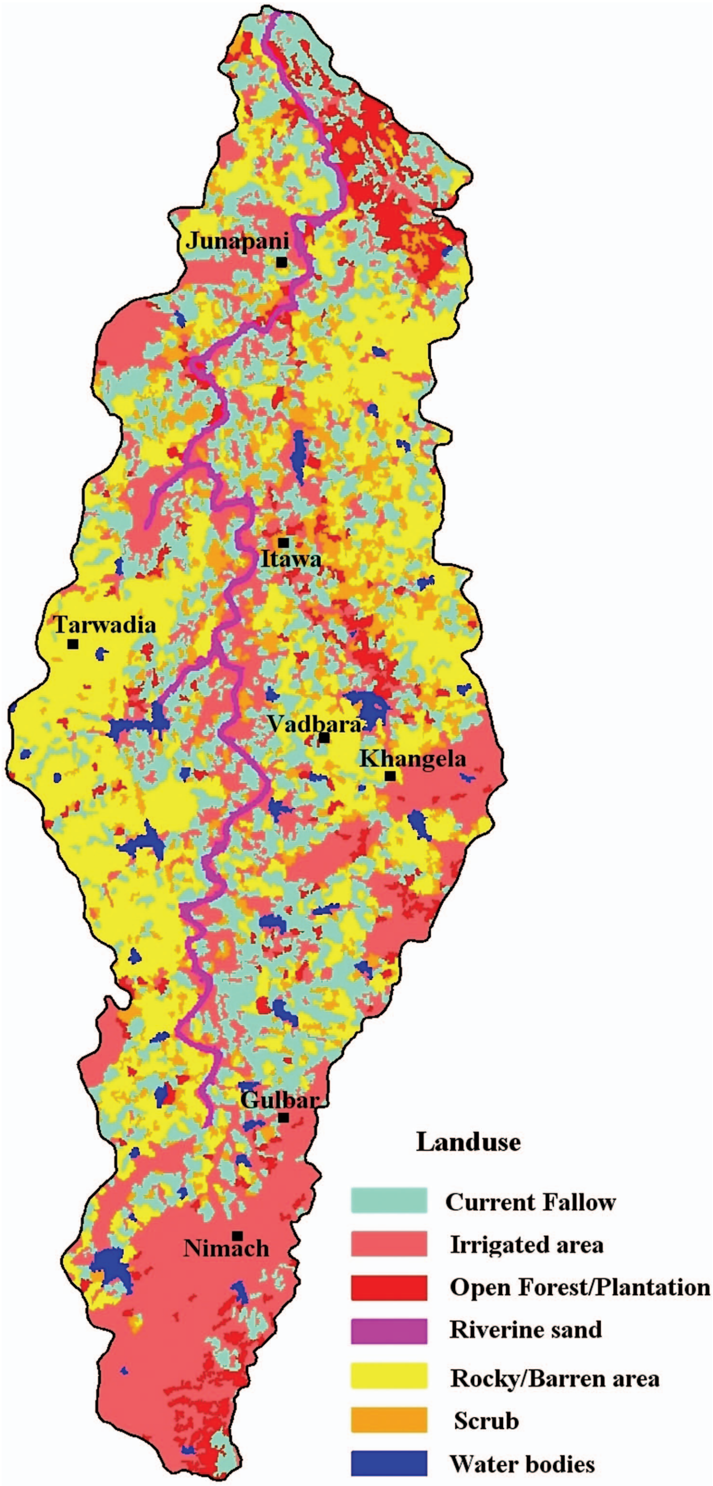

Figure 5. Land use/land cover map. Available in colour online.

rainfall exceeds the evapotranspiration and in dry seasons, the evapotranspiration exceeds the precipitation in that month. The severity of the dry season increases during subsequent months with excessive potential evapotranspiration. This was expressed as a cumulative, negative *P-PET* differential for the entire dry season. For the given period of analysis, the estimation of the *P-PET* differential was computed commencing from the end of a wet season until the end of the next wet season. In the drought period, the deficiency between *P* and *PET* would be initially compensated for by the soil water. However, as the evapotranspiration falls below the potential rate (as the soil dries) it is necessary to choose the functional relationship between the available water capacity and the potential water loss from the soil. Established empirical relations between water retained in the soil and accumulated potential water loss for different soils with different available water capacities and rooting depths (Dunne and Leopold 1978) were used herein. In the present study, the soil moisture status for each month with evapotranspiration exceeding precipitation was computed by

$$SM = W\exp(L_a/W) \tag{6}$$

Where SM is the soil moisture (mm), L_a is the accumulated potential water loss (mm) and W is the water capacity (mm).

Soil moisture values for the wet season were obtained by adding the excess precipitation, after meeting *PET*, to the soil moisture level at the end of the previous dry season. However, the soil can hold moisture only up to its holding capacity (water capacity). Hence, the soil would be at its water capacity throughout the wet months. Surplus water, which cannot be held in the soil by capillary and osmotic forces drains out of the root zone.

Whenever precipitation exceeds *PET*, the actual evapotranspiration (*AET*) was considered as equivalent to *PET*. When the meteorological demand was partially satisfied from the stored soil water, *AET* is the sum of precipitation (*P*) and the amount of soil moisture withdrawn from the storage. The amount by which the *AET* and *PET* differ in any month is called the soil moisture deficit. The excess amount of water that cannot be stored in the soil is termed as the moisture surplus.

Table 2. Runoff potential estimates for different landuse and hydraulic soil group (HSG) classes.

Land use	HSG	Rooting depth (m)	Available water capacity (%)	Σ Rainfall (mm)	Σ AET (mm)	Σ Runoff (mm)
Open forest	C	2	20	1256	1029	227
	D	1.17	30	1400	1137	263
Fallow	A	0.5	10	1256	760	496
	B	0.5	20	1256	720	536
	C	0.5	30	1256	657	599
Irrigated	A	0.5	10	1256	866	391
	B	0.5	20	1256	816	440
	C	0.5	30	1256	717	539
Barren	C	0.5	10	1256	648	608
	D	0.25	30	1400	742	658

AET, actual evapotranspiration.

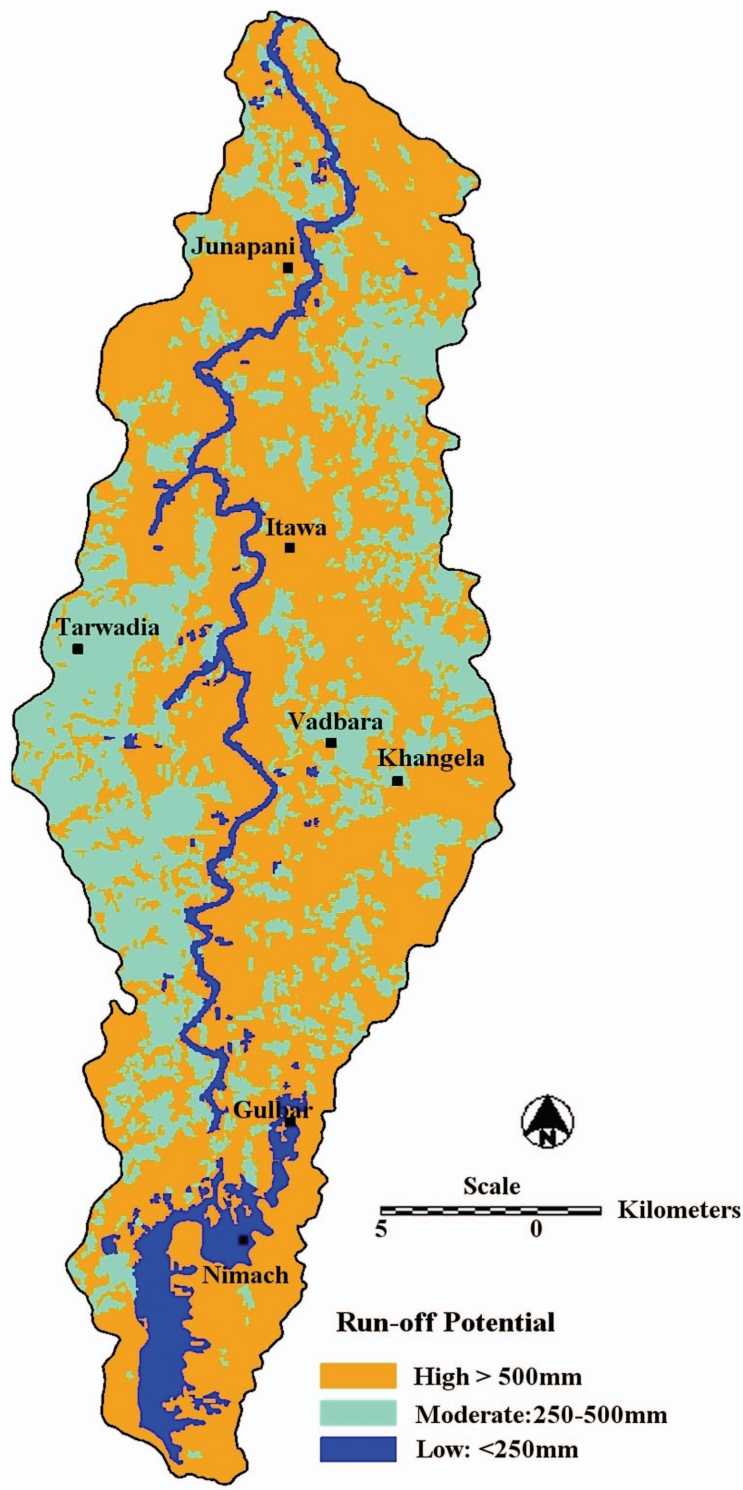

Figure 6. Classified runoff potential map. Available in colour online.

The moisture surplus drains to the ground water and eventually to streams. The fraction, which will leave a river basin as runoff, varies with the depth and texture of the soil and the physiography of the basin. Thornthwaite and Mather (1955) evaluated that approximately 50% of the surplus water alone is available for runoff in any month and the rest of the surplus drains into the subsoil, ground water, small lakes and channels of the basin and is available for runoff during the next month. Accordingly, runoff potential was evaluated for different land use classes and hydraulic soil groups (table 2).

4.7 *Runoff potential*

The runoff potential map (figure 6) was generated by integrating information on rainfall, land use, hydraulic soil groups and computed runoff values (table 2). As expected, barren/rocky areas with soil group class D amounts to maximum runoff potentiality (658 mm). The combination of open forest with soil group class C contributes the least runoff potential (227 mm). In the case of current fallow and irrigated landuse classes, the runoff varies from 391 mm to 591 mm, depending upon the soil type and rooting depth of the plants. On the basis of histogram distribution, the runoff potential map was classified into three classes, namely high (>500 mm), medium (251–500 mm) and low (<250 mm).

4.8 *Decision support*

An analytical hierarchy process (Saaty and Vargas 1991) was followed in assigning weight to different geo-technical parameters that influence site performance for water harvesting/recharging structures. In all, four parameters (slope, HSG, land use and discontinuities) were considered (table 3). Since the terrain comprises mainly

Table 3. Hierarchy of weights assigned for parameters governing site suitability.

Parameter	Overall weight	Category	Weight
Slope	54.3	Very steep (>35%)	30
		Moderately steep (15–35%)	27
		Strong (10–15%)	14
		Moderately strong (5–10%)	13
		Gentle (3–5%)	08
		Very gentle (1–3%)	05
		Nearly level (0–1%)	03
HSG	21.7	HSG D	57
		HSG C	29
		HSG B	09
		HSG A	04
Land use	10.8	Barren	56
		Fallow	27
		Irrigated	10
		Forest	05
Structure	13.1	1 set of discontinuity	64
		2 sets of discontinuity	28
		3 sets of discontinuity	07

HSG, hydraulic soil group.

hard and massive rocks, the discontinuity (joints, bedding planes, faults) was incorporated in lieu of lithology. The computation of a pairwise matrix, priority vector, eigenvalue and consistency ratios were derived for individual parameters and sub-classes of each parameter. In all the cases, the consistency ratio (CI/CR) was less than 0.09. Hence, weight assigned can be accepted with a high degree of confidence.

4.9 Site identification

By integrating all the thematic layers and weightage values, a composite map was generated in ARCInfo environment. On this map, site suitability analysis for check dam, percolation pond, subsurface dyke and farm pond was carried out by running queries using the decision tree concept. The resultant map (figure 7) is designated herein as the potential site suitability map.

In the field, suitable sites for these structures were identified following the IMSD (1995) and FAO (1977) guidelines (table 4). To understand the accuracy of estimation, an attempt was made to correlate the remote sensing derived (potential site suitability) map and field based site suitability map for a small micro-watershed area (figure 7). It was evident from proximity analysis that, in 75% of cases (out of 24 sites), the sites derived (for check dam/percolation pond, subsurface dyke) fall

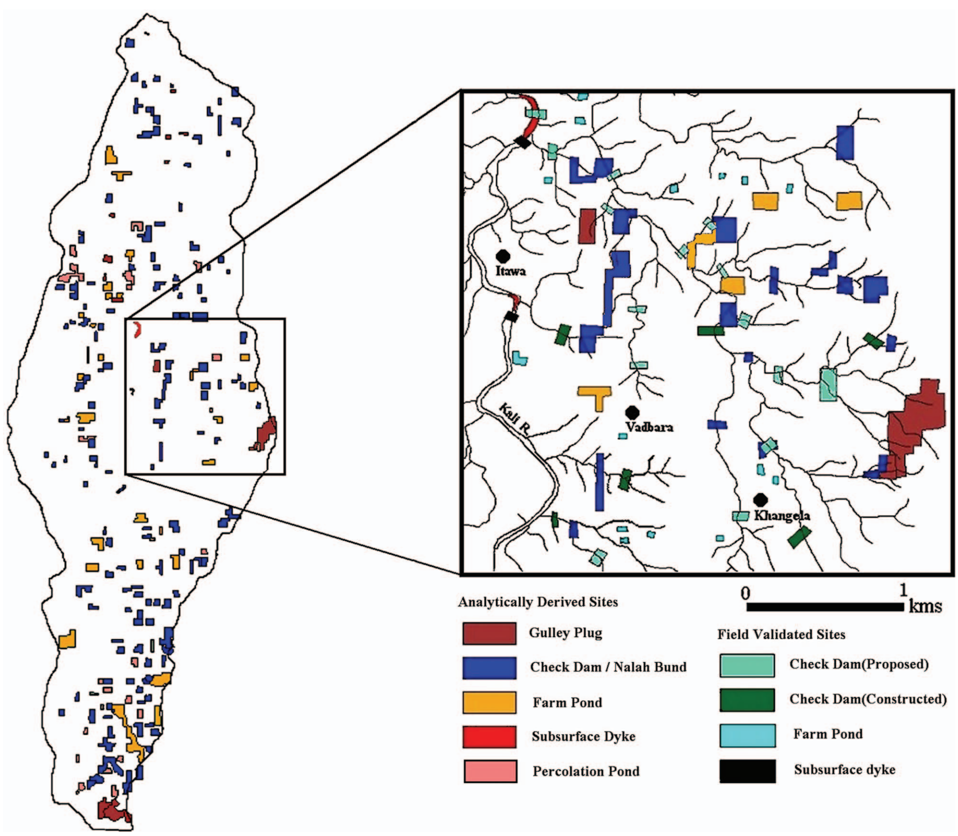

Figure 7. Potential site suitability map. Available in colour online.

Table 4. Adopted specifications for water harvesting/recharging structures.

Structure	Slope (%)	Porosity and permeability	Runoff potential	Stream order	Catchment area ($\times 10^4$ m^2)
Farm ponds	0–5	Low	Medium/high	1	1–2
Check dams	<15	Low	Medium/high	1–4	>25
Subsurface dyke	0–3	High	Medium/low	>4*	>5
Gully plug	15–20	Low	High	1	–
Percolation pond	<10	High	Low	1–4	25–40

*Ideally suited where evapotranspiration is high.

within 15 m distance of field identified sites. In 25% of cases, the suitable sites were within 35 m distance. This error can be attributed to a coarser scale of mapping (1:50 000) of different thematic layers.

The accuracy of estimation was higher (87%) in case of gulley plugs and farm ponds. However, in this case, field based site selection procedure is more appropriate by virtue of the following factors.

1. The remote sensing technique delineated fairly larger areas as suitable sites. But, field implementation requires very specific sites.
2. Conventionally, slope and area of overland flow were considered as the main factors governing site suitability of gulley plugs and farm ponds. In the present case, the digital elevation model (DEM) prepared at 1:50 000 scale is insufficient to delineate the gullies and gorges less than 20 m elevation.

5. Conclusion

Micro-watershed development calls for structural and biological remedies so as to augment water resources and minimize soil loss. In this study, a set of criteria was evolved to locate suitable sites for water harvesting/recharging structures. The criteria chosen were comprehensive and sensitive. The remote sensing technique proved to be effective for generating various thematic layers relevant to site suitability. GIS has facilitated in database management, analysis and derivation of results.

Acknowledgements

The authors are thankful to Dr P.S. Roy, Director, Indian Institute of Remote Sensing (IIRS), Dehradun, India, for his help in providing satellite data and computing facilities.

References

Cosh, M.H., Jackson, T.J., Bindlish, R. and Prueger, J.H., 2004, Watershed scale temporal and spatial stability of soil moisture and its role in validating satellite estimates. *Remote Sensing of Environment*, **92**, 427–435.

Dunne, T. and Leopold, L., 1978, *Water in Environmental Planning* (San Francisco, CA: W.H. Freeman and Company).

FAO, 1977, Guidelines for Watershed Management, *FAO Conservation Guide No.1* (Rome: FAO), 293 p.

HORTON, R.E., 1945, Erosional development of streams and their drainage basins: hydrophysical approach to quantitative morphology. *Geological Society of America Bulletin*, **56**, 275–370.

IMSD, 1995, *Integrated Mission for Sustainable Development: Technical guidelines* (Hyderabad: NRSA).

OUATTARA, T., GWYN, Q.H.J. and DUBOIS, J.M.M., 2004, Evaluation of the runoff potential in high relief semi-arid regions using remote sensing data: application to Bolivia. *International Journal of Remote Sensing*, **25**, 423–435.

PRASAD, K.S.S., GOPI, S. and RAO, R.S., 1993, Watershed prioritization using remote sensing techniques—a case study of the Mahabubnagar district, Andhra Pradesh, India. *International Journal of Remote Sensing*, **14**, 3239–3247.

SAATY, T.L. and VARGAS, L.G., 1991, *The Logic of Priorities/Analytical Planning (Analytical Hierarchy Process)*, 299 pp. (Pittsburgh, PA: RWS. Publications).

THORNTHWAITE, C.W. and MATHER, J.R., 1955, *The Water Balance*, vol. 8 (Centerton, NJ: Laboratory of Climatology).

YUSOF, K.W., SERWAN, M. and BABAN, J., 2000, Identifying optimum sites for locating reservoirs employing remotely sensed data and geographical information systems. *Proceedings of the 21 Asian Conference on Remote Sensing*, 4–8 December 2000, Taipei. http://www.gisdevelopment.net/aars/acrs/2000/ts2/water0001.asp